AN INTERMITTENT FREE-VIBRATION MEMS GYROSCOPE ENABLED BY CATCH-AND-RELEASE MECHANISM FOR LOW-POWER AND FAST-STARTUP APPLICATIONS

Ryunosuke Gando[1], Haruka Kubo[2], Yasushi Tomizawa[1, 3], Etsuji Ogawa[1], Shunta Maeda[1], Kei Masunishi[2], Yohei Hatakeyama[1], Tetsuro Itakura[1], and Tamio Ikehashi[1]

[1]Corproate Research & Develop Center, Toshiba Corporation, Japan

[2]Corporate Manufacturing Engineering Center, Toshiba Corporation, Japan

[3]Device & System Platform Development Center, Japan

ABSTRACT

This paper presents the first intermittent free-vibration MEMS gyroscope enabled by a "Catch-and-Release (CR)" drive mechanism, which realizes substantial power reduction and fast startup compared to existing stationary gyroscopes. In this architecture, the proof mass is captured at the maximum displacement position (catch-state), and then released to free vibration during which the Coriolis detection is performed (release-state). Thanks to the high quality factor (Q) of 72000, the released mass can be re-captured before attenuation. This CR mechanism enables instant startup and low power. The functionality and sensitivity (21.2 μV/dps) of a prototype CR gyroscope (CR-G) are confirmed by experiments.

INTRODUCTION

The demand for MEMS vibratory gyroscopes [1] is rising in applications such as motion processing and pedestrian navigation [2]-[4]. Recently, low power consumption is required in wearable devices, especially in the virtual reality and augmented reality applications [2], [4]. However, current gyroscopes [3], [4] have large power consumption due to the stationary drive of the proof mass (Figure 1a).

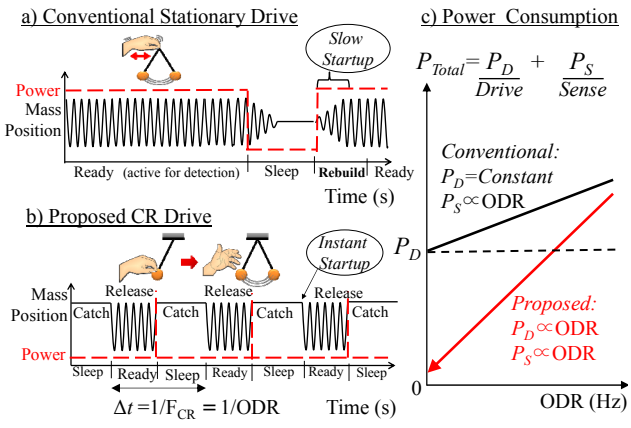

Figure 1: Concept comparison between the conventional stationary drive and the proposed intermittent catch-and-release (CR) drive.

In principle, the drive power can be reduced by intermittent mechanical operation instead of full-time operation. This, however, is not applicable to the conventional stationary drive scheme because of the additional startup time and power caused by amplitude rebuilding (Figure 1a). Furthermore, stationary gyroscopes require a close-loop control circuit to realize a stable drive-mode amplitude, which consumes substantial power [1], [3]-[4].

To address the power consumption issue, this paper presents a novel mechanism called the "Catch-and-Release (CR)" drive. The CR drive enables intermittent mechanical operation without the close-loop circuit.

DESIGN CONCEPT

The CR mechanism introduces a catch-state and a release-state enabled by the MEMS structure shown in Figure 2. It contains a DC-voltage-biased hold electrode that forms a parallel plate capacitor with the 0 V-biased mass electrode. An electrically floating stopper is inserted between the two electrodes to avoid electrical short and to define the capacitor gap of the catch-state. In the catch-state, the drive mass is electrostatically caught at the maximum amplitude by setting the hold-electrode voltage V_H to a catch voltage V_C. In the release-state, the free vibration starts immediately after V_H is set to 0 V. The Coriolis force applied to the free vibration mass is used to detect the angular velocity.

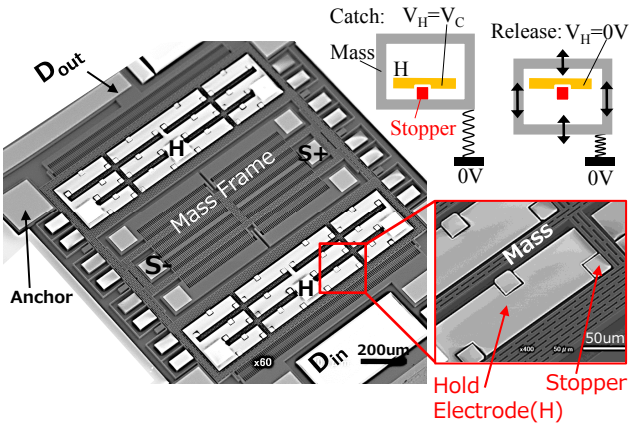

Figure 2: SEM picture of a prototype catch-and-release gyroscope (CR-G) and a cartoon of the CR operation with hold and stopper electrodes.

As shown in Figure 3, a synchronous demodulation using the output drive signal Dout is carried out to extract the Coriolis amplitude from the differential sense signals S+ and S-. The CR operation is repeated, and its frequency F_{CR} corresponds to the output data rate (ODR). As illustrated in Figure 1c, power reduction of the CR drive is prominent at the low ODR region.

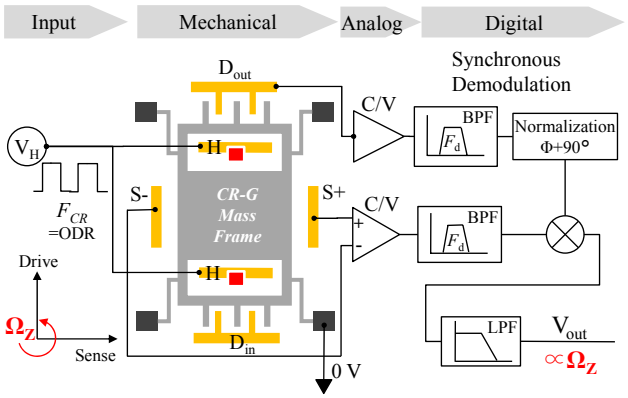

Figure 3: CR-G architecture and block diagram for a mode-split open-loop readout.

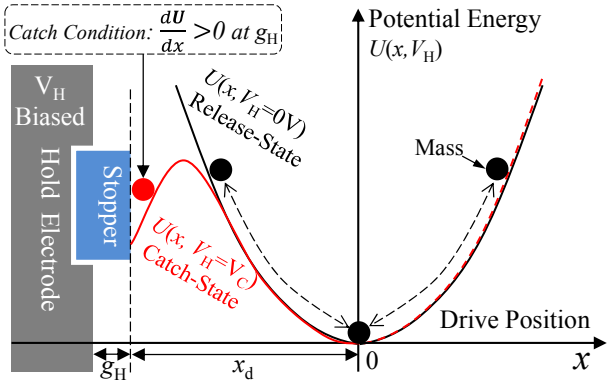

Figure 4: Potential energy conditions for the catch and release operations.

The physical condition of the catch operation can be derived from the potential energy curve of the mechanical and electrostatic system. As shown in Figure 4, when a voltage V_H is applied to the hold electrode, two forces are applied to the mass: the spring force that restores it to the original position and the electrostatic force that pulls it toward the stopper. The total potential energy can be written as a function of position x and V_H:

$$U(x,V_H)=\frac{kx^2}{2}-\frac{\varepsilon_0 S V_H^2}{2(x+x_d+g_H)}, \qquad (1)$$

where k, x_d, S, and g_H, are the spring constant, maximum amplitude, hold capacitor area, and the hold capacitor gap, respectively.

The mass would be trapped in the potential valley, i.e., the catch-state, when the condition $dU/dx > 0$ is met at the stopper position. Using equation (1), the catch condition is written in terms of V_C as

$$V_C > \sqrt{\frac{2\,k\,x_d g_H^2}{\varepsilon_0 S}} \equiv V_{CMIN} . \qquad (2)$$

Here V_{CMIN} is the theoretical minimum voltage to achieve the catch state.

FABRICATION AND IMPLEMENTATION

A prototype single-axis CR-G is designed following the concepts described in the previous section. The resonance frequency of drive (F_d) and resonance frequency of sense (F_s) are split for this CR-G. In the fabrication, a standard deep RIE process for an SOI wafer was employed, as shown in Figure 5. Detailed device parameters are listed in Table 1.

To evaluate CR-G, MEMS chips are mounted onto a custom PCB (Figure 6). Note that on this PCB, feedback control function to keep the drive resonance is not necessary, thanks to the CR drive mechanism. The readout architecture (Figure 3) is an open-loop one. The mass motions in the drive and sense directions are read through C/V converters with transimpedance amplifier. In the current measurement system, the drive and sense output waveforms are measured and stored with a digital oscilloscope. Digital signal processing including band pass filter and synchronous demodulation are performed on the stored data, using the MATLAB software.

Rotational experiments are carried out by attaching the PCB onto a turntable placed in a vacuum chamber, as shown in Figure 6. The pressure inside the vacuum chamber is set to 1 Pa.

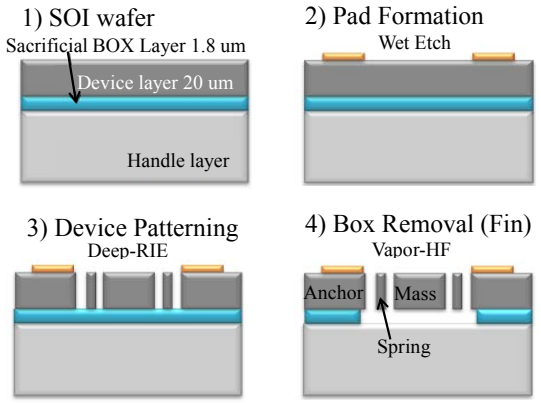

Figure 5: Cross-section view of process flow of a SOI-based bulk micromachining fabrication for CR-G.

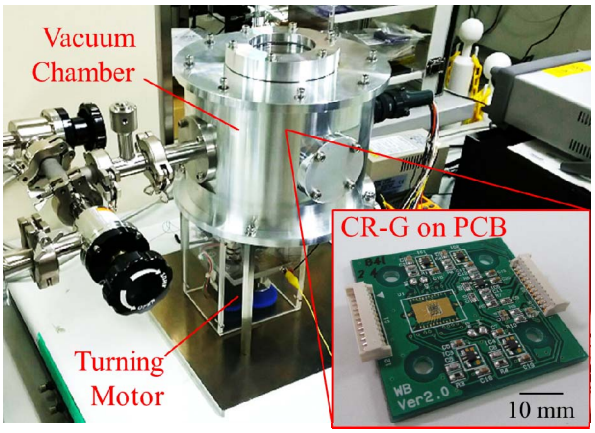

Figure 6: Vacuum chamber with turntable function and a prototype CR-G implemented on a custom PCB.

EXPERIMENTS AND RESULTS

CR-G requires an initialization step in which the mass is setup to the catch-state. This is done with the use of a resonant pull-in technique [5]. Firstly, an external sine wave with frequency at drive resonance of 11.5 kHz and AC amplitude of 5 V is applied at the Din electrode to boost the amplitude toward the stopper position (Figure 4).

Next, a DC voltage of 40 V as V_C is applied to the hold electrode H to capture the mass. To ensure the catch operation, the applied V_C is intentionally set higher than the theoretical minimum in equation (2), which is V_{CMIN} =36 V. It is possible to reduce the voltage V_C by lowering g_H or by increasing S as implied by equation (2).

After the initialization, the external sine wave is no longer necessary, and instead a square wave with the amplitude of V_C is applied intermittently to drive the CR-G. As shown in Figure 7, consecutive CR operations are confirmed at F_{CR}=100 Hz and Q=72000. The CR frequency F_{CR} is tunable and successful operations in a range from 5 Hz up to 2 kHz are confirmed.

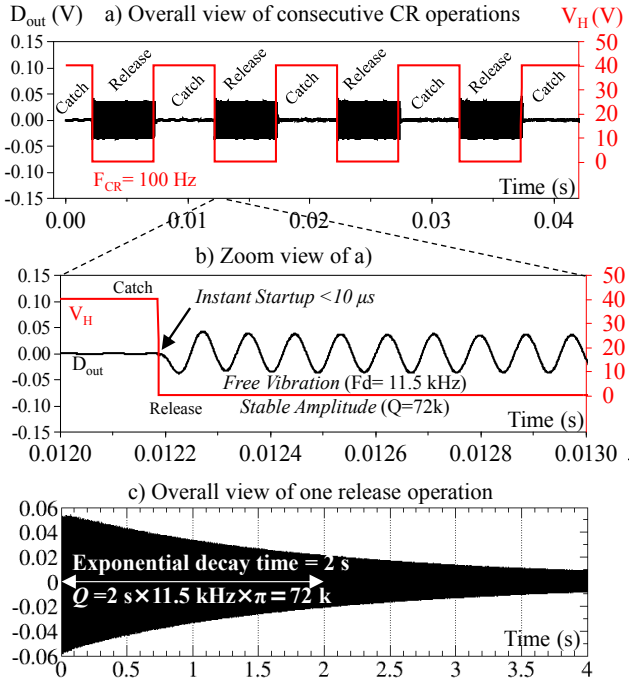

Figure 7: Measured waveform of a), b) consecutive CR operations, and c) one release operation acquired by an oscilloscope. Output signal Dout represents the mass motion proportional to the time variation of capacitance dC/dt.

The measured CR waveform shows that the mass vibration starts instantly after the release and reaches the maximum amplitude within the first oscillation circle. The observed startup time is less than 10 μs, which is in principle determined by the switching speed of the pulse generator. Thanks to the high Q factor, the free-vibration amplitude is stable with a decay time constant of 2 s (Figure 7c), which is suitable for the Coriolis detection. For the example in Figure 7, the release time is 5 ms, and the amplitude decrease is only 0.3 % before the recapture.

As shown in Figure 8, the sensitivity curve of the output voltage V_{out} (cf., Figure 3) for the z-axis input rotation rate is obtained from the tunable tests. The measured scale factor is 21 μV/dps. Good linearity of R^2=0.999 is observed in the range from 0 up to 700 dps. This scale factor is consistent with the designed values of the device capacitive sensitivity and the readout circuit gain.

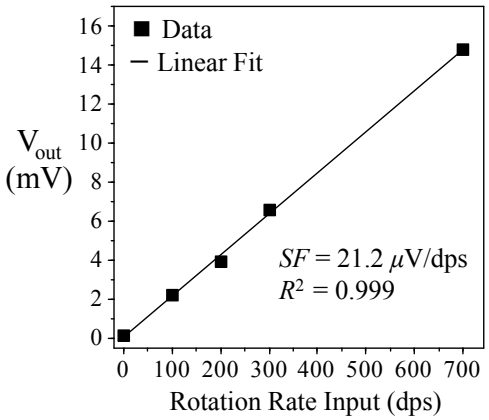

Figure 8: Sensitivity curve of output voltage against input rotation rate obtained the prototype CR-G. Note that dps stands for degree per second.

Table 1. Summary of device parameters.

Parameter	Value
Wafer	SOI (20 μm-thick Si)
Size	1.6 mm × 1.7 mm
Proof Mass	26 μg
Drive Resonance Freq. F_d	11.5 kHz
Sense Resonance Freq. F_s	15.0 kHz
Maximum Amplitude x_d	5 μm
Quality Factor Q	72000 at 1 Pa
Maximum Amplitude x_d	5 μm
Capacitance Gradient dC/dx	30 fF/μm
Scale Factor (split mode)	21.2 μV/dps
Rest Capacitance C_0 Drive /Hold /Parasitic	0.7 / 2 /1 pF
Catch-state Voltage V_C	40 V
Effective Catch-state Gap g_H	1.0 μm

DISCUSSION

In order to compare the CR drive with the conventional stationary drive, we discuss the theoretical models of power consumption and startup time, and quantitatively compare their differences.

Stationary Drive

In the stationary drive architecture [1], the mechanical vibration of proof mass is realized by excitation with electrostatic harmonic force F_{AC} (= kx_d/Q) at the resonance frequency F_d. The drive power of the MEMS corresponds to the mechanical loss,

$$P_{\text{STA, MECH}} = 2\pi \times F_d \times \frac{\frac{1}{2}kx_d^2}{Q} \quad . \qquad (3)$$

where the term $1/2kx_d^2$ is the potential energy stored at the spring, and Q is the effective mechanical quality factor that reflects the air damping, the thermo-elastic damping, and the anchor loss. Besides, electric power is consumed at charging and discharging the rest capacitor C_0 by an AC voltage used for the force generation. Here C_0 includes the base and parasitic capacitance of the MEMS.

On the other hand, the startup time after power-on and the recovery time from the sleep mode to the active mode (Figure 1a) is limited by the time constant of the mechanical amplitude rebuilding. The time constant is written as below [6],

$$\tau_{\mathrm{STA}} = \frac{Q}{F_{\mathrm{d}}\pi} \quad . \tag{4}$$

According to equation (3), the power consumption of stationary drive is proportional to the F_{d} and inversely proportional to the Q factor. It is difficult to reduce power by lowering F_{d} because it is typically designed to be larger than 10 kHz for commercial gyroscopes to avoid the environmental noise [3]. Alternatively, the power loss can be reduced by increasing the Q factor. This approach, however, has a trade-off with the startup time as indicated by equation (4).

CR Drive

In the CR drive architecture with a high Q factor, the mechanical power loss is negligible. The drive power is mainly the electric loss on charging and discharging the rest capacitor C_0 by the catch voltage V_{C},

$$P_{\mathrm{CR,\ ELEC}} = \frac{1}{2} C_0 {V_C}^2 \times F_{\mathrm{CR}} \quad . \tag{5}$$

where the term $1/2C_0V_C^2$ is the electrostatic energy stored at the capacitor for each circle. It is possible to reduce the power by lowering V_{C} or the CR operation frequency F_{CR}. Unlike the stationary drive, the startup time of CR-G is not affected by the high Q factor, which is less than 10 μs as shown in Figure 7b.

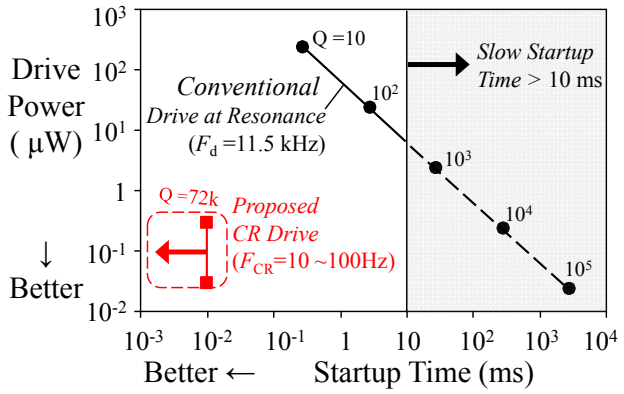

Figure 9: Drive-power vs. startup-time plot for the conventional stationary drive and the CR drive on the same MEMS device (cf., parameters in Table 1).

From the above analyses and equations, we estimated the drive power and the startup time using the same device parameters obtained from measurements (see Table 1). As indicated by the scatterplot of Figure 9, the CR drive is free from the tradeoff between low power (high Q) and long startup time, which is inevitable in the conventional scheme. In the present approach, the startup time is negligible, and the drive power can be reduced by 1 order of magnitude, compared to the case of startup time below 10 ms and F_{CR} (=ODR) below 100 Hz.

CONCLUSIONS

We designed and fabricated a prototype CR gyroscope (CR-G) operating in intermittent free vibration. The drive circuit of CR-G is a simple open-loop one because it requires no feedback control. The functionality and sensitivity are experimentally demonstrated. The superior performances over the conventional stationary gyroscopes with respect to low power consumption and fast startup are shown quantitatively. Future works will be focused on design extension toward the 3-axis CR-G, sensitivity optimization for the noise performance, and further power reduction by optimizing the CR electrode structure.

ACKNOWLEDGEMENTS

We appreciate K. Ikeda of AC Technologies Co., Ltd for supports in making the evaluation board. This work is partially based on results obtained from a project commissioned by the New Energy and Industrial Technology Development Organization (NEDO).

REFERENCES

[1] C. Acar and A. Shkel, “MEMS Vibratory Gyroscope”, in *MEMS Reference Shelf, Springer*, ISBN 978-0-387-09535-6, 2009

[2] Gerhard Lammel, “The Future of Mems Sensors in Our Connected World”, in *Digest Tech. Papers, MEMS 2015 Conference*, pp. 61-64

[3] L. Prandi et al.,” A Low-Power 3-Axis Digital-Output MEMS Gyroscope with Single Drive and Multiplexed Angular Rate Readout”, in *Digest Tech. Papers, ISSCC 2011*, pp. 104-106

[4] C. D. Ezekwe et al., “A 3-Axis Open-Loop Gyroscope with Demodulation Phase Error Correction”, in *Digest Tech. Papers, ISSCC 2015*, pp. 478-580

[5] A. Fargas-Marques et al., “Resonant Pull-In Condition in Parallel-Plate Electrostatic Actuators”, in *JOURNAL OF MICROELECTROMECHANICAL SYSTEMS, 2007*, vol.16, no. 5, pp.1004-1053

[6] N. Yazdi, F. Ayazi, and K. Najafi, "Micromachined Inertial Sensors" *in Proc. of the IEEE, Aug. 1998*, vol. 86, no. 8, pp.1640-1659,.

CONTACT

*Ryunosuke Gando, tel: +81-44-549-2856;
ryunosuke.gando@toshiba.co.jp